RSC Advances

ROYAL SOCIETY OF CHEMISTRY

www.rsc.org/advances

Influence of the Double Bond on the Hydrogen Abstraction Reactions of Methyl Esters with Hydrogen Radical: an Ab Initio and Chemical Kinetic Study

Quan-De Wang[a,*], Weidong Zhang[b]

[a]Low Carbon Energy Institute, China University of Mining and Technology, Xuzhou 221008, Jiangsu, People's Republic of China

[b]Wuhan Institute of Marine Electric Propulsion, CSIC, Wuhan 430064, Hubei, People's Republic of China

*Corresponding author. Email address: wqd198686@126.com (Q.-D. Wang)

Abstract: This work reports a systematic *ab initio* and chemical kinetic study of the rate constants for hydrogen atom abstraction reactions by hydrogen radical on the isomers of unsaturated C6 methyl esters. Geometry optimizations and a frequency calculations s of all of the species involved, as well as the hindrance potential descriptions for reactants and transition states have been performed at the B3LYP/6-311G(2d,d,p) level of theory implemented in the composite CBS/QB3 method. The intrinsic reaction coordinate (IRC) calculations are performed to verify that the transition states are the right minima connecting the reactants and the products. The hindered rotor approximation has been used for the low frequency torsional modes in both reactants and transition states. The high-pressure limit rate constants for every reaction channel in certain methyl ester fuel molecules are calculated via conventional transition-state theory with the asymmetric Eckart method for quantum tunneling effect by using the accurate potential energy information obtained with the CBS/QB3 method. The individual rate constants at different reaction sites for all the methyl esters in the temperature range from 500 to 2500 K are calculated and fitted to the modified three parameters Arrhenius expression using least-squares regression. Further, a branching ratio analysis for each reaction site has also been investigated for all of the methyl esters. To the best our knowledge, it is the first systematic theoretical studies to investigate the influence of the double bond on the elementary reaction kinetics of methyl esters. This work not only provides accurate reaction rate coefficients for combustion chemical kinetic modeling, but also helps to gain further insight into the combustion chemistry of biodiesel in future investigations.

Keywords: Hydrogen abstraction reactions; Transition state theory; Double bond; Unsaturated methyl esters

1. Introduction

Biodiesel fuels are renewable alternatives to conventional fossil fuels and the recent large amounts of utilization of biodiesel are motivating intense research efforts to achieve a comprehensive understanding of biodiesel combustion chemistry.[1] Biodiesel fuels are primarily comprised of alkyl esters, whcih are derived from plant oils or animal fats via the esterification process.[2] Most biodiesel fuels contain both saturated and unsaturated esters, with the size and relative abundance of the individual esters dependent on the feedstock. Many investigations have been performed to study combustion related processes of biodiesel and surrogates, most of which are saturated methyl esters and ethyl esters.[3-4] It is found that unsaturated esters also have been found to be important intermediates in the oxidation of large biodiesel fuels. Unsaturation in biodiesel esters not only affects the combustion properties and engine performances, but also influences the particulate matter emissions as well as the NO*x* emissions.[3-5] Therefore kinetic investigations on unsaturated methyl and ethyl esters are important and necessary to reveal the impact of C=C double bond on the combustion chemistry of relevant processes.

A limited number of studies have been performed to understand the effect of the double bond in biodiesel molecules on the combustion properties. Initially, to provide insights into the combustion chemistry of practical biodiesel fuels, short-chain alkyl esters containing functional groups similar to those in practical biodiesel fuels have been investigated using many experimental facilities and kinetic modeling. Sarathy et al. performed oxidation experiments of a saturated (methyl butanoate) and an unsaturated (methyl crotonate) C4 esters in opposed flow diffusion flames and jet stirred reactors (JSR).[6] Further, Gaïl et al. obtained new experimental results in JSR and modeled the related combustion processes by using a detailed chemical kinetic mechanism.[7] Using tunable synchrotron vacuum ultraviolet (VUV) photo-ionization mass spectrometer, Yang et al. investigated the detailed chemical structures of low-pressure premixed laminar flames of three simple unsaturated $C_5H_8O_2$ esters and the experimental results are modeled via a detailed chemical kinetic mechanism. They concluded that the C=C double bond enhanced the formation of oxygenated intermediates and other unsaturated components.[8] Zhang et al. performed experimental and kinetic modeling study of an unsaturated C6 ester (i.e., *trans*-methyl-3-hexenoate) in JSR, and the results were compared to the saturated ester methyl hexanoate.[9] The sooting tendencies of twenty C4 to C7 unsaturated esters in nonpremixed flames were also studied recently by Das et al. to better understand the effect of these double bonds on the sooting properties of esters.[10]

The limited number of studies on small unsaturated esters forms an important foundation to develop

detailed chemical kinetic reaction mechanism and model the combustion of real large biodiesel fuels. In 2010, Herbinet et al. developed detailed chemical kinetic mechanisms to study the oxidation of two large unsaturated esters: methyl-5-decenoate and methyl-9-decenoate.[11] The modeled results were compared with a rapeseed oil methyl esters oxidation experiments. It was observed that methyl-5-decenoate shown lower reactivity than methyl-9-decenoate and this was ascribed to more difficult isomerization process over the double bond. Further, Westbrook et al. conducted a series of research on the effects of unsaturation on the combustion properties of biodiesel fuels via detailed modeling studies by employing relatively comprehensive detailed chemical kinetic mechanisms.[12-14] In a more recent work, they investigated the effects of C=C double bond on the ignition of biodiesel fuels and it was concluded that the double bond reduces low temperature reactivity due to the reductions in cetane numbers because of the C=C double bond.[14] Most recently, Fridlyand et al. performed single pulse shock tube experiments to investigate the effect of the alkyl chain structure on the high pressure and temperature oxidation of a representative unsaturated biodiesel, namely, methyl nonenoate. The experimental results were modeled via chemical kinetic mechanisms generated by Reaction Mechanism Generator. It was concluded that significant uncertainties exist in the chemistry of unsaturated esters with the double bonds located close to the ester groups.[15] Therefore, further refinements of important elementary reactions are badly needed to improve the predictive abilities of detailed chemical kinetic mechanisms.

Under combustion relevant conditions, hydrogen atom abstraction reactions by small radicals (H, OH, O, HO_2, and CH_3) from fuel molecules are always important in the oxidation of fuels.[16-17] Although a series of theoretical and kinetic studies have been performed on the elementary reactions of saturated esters,[18-24] however, little attention has been given to obtain a better understanding of the effect of the double bond on the elementary reaction kinetics of methyl esters. In particular, the hydrogen abstraction reactions by H radical for methyl esters, which are one of the major fuel consumption pathways during oxidation, are not well understood at combustion relevant conditions. Therefore, to provide fundamental insight into the impact of C=C double bond on the hydrogen abstraction reactions, a systematic *ab initio* and chemical kinetic study of the rate constants for hydrogen atom abstraction reactions by H radicals on the isomers of unsaturated C5 methyl esters has been performed. This paper is organized as follows. Section 2 details the computational methods. Section 3 is devoted to the discussions of computational results, and the main conclusions are presented in section 4.

2. Computational details

In order to investigate the effect of the C=C double bond on the hydrogen abstraction reaction kinetics of methyl esters, three saturated C6 methyl esters, namely, methyl valerate, methyl 2-methylbutanoate, methyl

isopentanoate together with their corresponding unsaturated esters with a single C=C double bond located at different positions are investigated. Figure 1 shows the different types of hydrogen atoms and the labels uses for the three saturated C6 methyl esters in this work. The structures of all the esters are listed in table 1. All of the electronic structure calculations are carried out with the Gaussian 09 program.[25] The composite CBS-QB3 method[26] is applied for all the species including the reactants, transition states, and products. The CBS-QB3 model involves a five-step calculation starting with a geometry optimization and a frequency calculation (scaled by a factor 0.99) at the B3LYP/6-311G(2d,d,p) level of theory, followed by single point energy calculations at the CCSD(T)/6-31G(d'), MP4SDQ/cbsb4, and MP2/cbsb3 and a complete basis set extrapolation to correct the total energy. Analytical harmonic frequency calculations are performed at the same level to obtain the zero-point energy and thermo-corrections and to confirm the existence of transition states with one and only one imaginary frequency and other stationary geometries corresponding to the true local minimum with no imaginary frequency. The intrinsic reaction coordinate (IRC) calculations[27] are performed to verify that the transition states are the right minima connecting the reactants and the products. All calculations are performed by using the unrestricted open-shell calculation without spin-orbit corrections.

The description of thermodynamic properties and reaction kinetics involving large aliphatic chains requires an accurate treatment of low-frequency internal rotations. Using the traditional harmonic oscillator (HO) approximation to describe these internal rotation modes can lead to large errors in the partition function. In this work, low frequency internal rotations are treated as hindered rotors.[28-30] Specifically, the potentials of each internal rotation of all methyl esters are calculated at the B3LYP/6-311G(2d,d,p) level of theory using a relaxed energy scan. The resulting potential energies as a function of the dihedral angle, $V(\phi)$, are fitted to a Fourier series, e.g., $V(\phi) = \sum_{m=0}^{5} A_m \cos(m\phi) + B_m \sin(m\phi)$. The reduced moment of inertia $I^{(2,3)}$ of the equilibrium geometry is computed and the resulting one-dimensional Schrodinger equation is solved for the lowest 200 energy levels. These energies are substituted into the canonical partition function, which are used to calculate the thermodynamic quantities. The fitting to the Fourier series, the calculation of $I^{(2,3)}$ and solving the one-dimensional Schrodinger equation are carried out using Cantherm.[31] For transition states, the potentials of hindered internal rotations closest to the reaction centers are also computed at the B3LYP/6-311G(2d,d,p) level of theory using a relaxed energy scan but with the bond lengths at the critical geometries frozen, while the properties for the other hindered internal rotations employ the scan results for the corresponding methyl esters.

For methyl esters, the thermodynamic properties including the enthalpy of formation and entropy at 298 K

and the heat capacity at the following temperatures: 300, 400, 500, 600, 800, 1000, and 1500 K are calculated. High-pressure limit rate constants for all the hydrogen abstraction reactions investigated in this work are calculated according to conventional transition state theory (TST),[32]

$$k(T) = \kappa(T)\sigma \frac{k_B T}{h} \frac{Q^{\mathrm{TS}}(T)}{Q^{\mathrm{Reacts}}(T)} \exp(-E_a / RT) \qquad (1)$$

in which $\kappa(T)$ is known as the transmission coefficient to account for the quantum tunneling effects, and σ is the reaction symmetry number. $Q^{\mathrm{TS}}(T)$ and $Q^{\mathrm{Reacts}}(T)$ represent the total partition function of the transition state and the reactants. E_a is the classical barrier height, namely, the difference between the electronic energies of the transition state and the reactants. The hindered rotor approximation developed by McClurg et al. has been adopted for the treatment of internal rotations during the calculation of reaction rate constants. All the rate constant calculations are performed using KiSThelP software.[33] The rate constants are calculated at temperatures from 500 to 2500 K in increments of 50 K, and the data are fitted to the modified Arrhenius expression using least-squares regression, $k(T) = AT^n \exp(-E_a / RT)$, in which A is the Arrhenius prefactor, T is the temperature, E_a is the barrier height, and n is the temperature exponent indicating the deviation from the standard Arrhenius equation.

3. Results and discussion

3.1. Reaction enthalpies and energy barriers

For all the methyl esters, table 1 lists the calculated the enthalpy of formation and entropy at 298 K and the heat capacity at the following temperatures: 300, 400, 500, 600, 800, 1000, and 1500 K. The standard enthalpy of formation at 298 K is calculated with the atomization energy scheme.[34] For methyl valerate, the calculated value of standard enthalpy of formation at 298 K is -113.4 kcal/mol, which is in good accordance with experimental results with a small deviation of 0.6 kcal/mol. For methyl 2-methylbutanoate and methyl isopentanoate, from table 1, it can be seen that the deviations between the calculated results and the experimental results are larger than that of methyl valerate. However, the experimental results have an uncertainty of 1.8 kcal/mol. Considering the CBS-QB3 method still has an uncertainty of 1~2 kcal/mol in the enthalpy of formation, the calculated results are also in good agreement with experimental values, indicating the high accuracy of the CBS-QB3 method used in the present work. From table1, it can be seen that the existence of the C=C double bond greatly increases the standard enthalpy of formation of the corresponding

saturated methyl esters, while the influence on the entropy is small and irregular. For heat capacity, the influence of the C=C double bond increases as the temperature raises.

The uncertainty of the predicted theoretical rate constants significantly rely on that of the calculated barrier height. A few theoretical methods have been demonstrated to be effective and accurate for organic molecules that are of interest to combustion chemistry. For example, the CCSD(T) and QCISD(T) methods within the framework of coupled cluster theory combined with an extrapolation to complete basis set (CBS) can yields the predictions of barrier heights and reaction enthalpies to be accurate to around 1.0 kcal/mol.[17, 35-36] Unfortunately, these methods are computationally expensively and haven't been applied to a system with more than 10 non-hydrogen atoms. For large systems that of interest in combustion chemistry, the composite methods such as the CBS-QB3 method used in this work provide an effective way to obtain accurate barrier heights and reaction enthalpies. First of all, the accuracy of the CBS-QB3 method is validated via comparisons of the calculated results with previous works. To the best of our knowledge, very fewer studies have been performed on large methyl esters with more than 5 carbon atoms except the recent high-level theoretical studies by Zhang et al.[37] Table 2 lists the calculated energy barrier heights and reaction enthalpies for methyl valerate in this work and the results by Zhang et al.[37] From table 2, it can be seen that the predicted barrier heights and reaction enthalpies for methyl valerate in this work are in excellent agreement with the results at the high-level QCISD(T)/CBS method.[37] The deviations of energy barriers and reaction enthalpies are less than 0.34 and 0.8 kcal/mol, respectively, indicating the high efficiency of the CBS-QB3 method used in the present work.

Theoretical predicted energy barriers and reaction enthalpies for all methyl esters at different reaction sites are listed in table 3. From table 3, it is obvious that effect of the C=C double bond and the chain branching on the barrier heights and reaction enthalpies at the α' site is small. Through a detailed comparisons of the predicted barrier heights and reaction enthalpies at different reaction sites for methyl valerate, methyl 2-methylbutanoate, and methyl isopentanoate, it can be found that predicted barrier heights exhibit the following tendency: primary carbon (from 10.1 to 10.4 kcal/mol) > secondary carbon (from 6.8 to 7.6 kcal/mol) > tertiary carbon (from 5.3 to 6.7 kcal/mol), while the reaction enthalpies still show the same tendency but the actual values change bigger than that of barrier heights. Specifically, the reaction enthalpies at the methoxy group (α' site) don't change greatly, even though considering the effect of C=C double bond. However, the reaction enthalpies for the secondary and tertiary carbon vary larger at different reaction sites. For all the other methyl esters with C=C double bond, it is obvious that the hydrogen abstraction reaction at the C=C double bond position is difficult due to the high barrier heights. However, reactivity on the allylic sites

with the presence of the C=C double bond increases and the barrier heights are the smallest among all the reaction sites. The calculated reaction enthalpies also reveal the same tendency.

For the development of detailed combustion reaction mechanisms, a linear energy relationship (LER) between barrier height and reaction energy, similar to the well-known Evans-Polanyi-like relationships is very useful. Figure 2 shows the LER between the barrier heights and reaction enthalpies at 298 K for the H-abstraction reactions of all the methyl esters with H in this work. The trend of the barriers can be described by $\triangle E_{barrier}$= 11.77631 + 0.33264$\triangle H_{enthalpies}$ with a Adj. R-Squared of 0.88. Such LER expressions can be helpful to quickly estimate the kinetic parameters of reactions in the same reaction class for large ester fuels.

3.2. High-Pressure limit rate constants

Another main objective of this study lies in the determination of the high-pressure limit rate constants of the hydrogen abstraction reactions by the H radical on the above methyl esters based on the above potential energy surfaces. The high-pressure limiting rate constants for the studied reactions are calculated by conventional TST according to eq 1.

Based on previous studies on the hydrogen abstraction reactions by the H radical, tunneling is important at lower temperatures (500-1100 K).[18-19] Tunneling coefficients can be accurately calculated via multidimensional tunneling methods.[38] However, these methods are too computationally demanding. Thus, the one-dimensional Eckart method[39-40] is widely used in theoretical combustion kinetics because it is rather inexpensive computationally yet accurate enough for the temperatures of interest in comparison to the small-curvature tunneling method, although such agreement is in fact fortuitous and caused by error cancellations.[41] Therefore, in this work, quantum tunneling effect is taken into account via the asymmetric Eckart method as implemented in KiSThelP. Figures 3 and 4 show the effect of the low frequency internal rotations and the tunneling effect on the calculated reaction rate constants at the α' site of methyl valerate. From figure 3, it can be seen that the effect of internal rotation on the rate constants increases as the temperature increases. Although the effect of internal rotation is small at low temperatures, the calculated rate constants can have a factor of 2 at high temperatures without the hindered rotor treatment. Compared with the internal rotations, the effect of tunneling mainly occurs at low temperature as shown in figure 4. It is also demonstrated that the modified three-parameter Arrhenius expression should be used to accurately describe the reaction rate constants instead of the standard Arrhenius formula in figure 4.

The accuracy of the calculated reaction rate constants are then validated via comparisons with previous theoretical calculations or experimental results. To the best of our knowledge, few studies have been performed

on the hydrogen abstraction reactions for C6 methyl esters, especially unsaturated methyl esters. However, based on previous studies, it is found that the length of the alkyl group in methyl esters does not affect the reactivity of H with methyl esters at the methoxy group (α' site). Therefore, the calculated rate constants at the α' site for methyl valerate have been compared with previous studies to validate the effectiveness of the adopted calculated methods and to confirm the reliability of the results. Figure 5 exhibits the calculated rate constants together with results from previous studies for methyl acetate and methyl valerate. The abstraction reaction at the α' site for methyl valerate and methyl acetate belongs to the same reaction class, and Wang et al.[18] have performed systematic theoretical studies for this reaction class employing reaction-class TST. It can be seen that the results obtained in this work are in good consistent with that from reaction-class TST. Most recently, Tan et al. employed very accurate theoretical methods to predict chemically accurate reaction energies for methyl acetate, and they also calculated the reaction rate constants. From figure 5, it can be seen that the results obtained in the present work can be as accurate as those from very accurate but very time-consuming theoretical methods, confirming the reliability of the present results.

Figures 6, 7 and 8 display the reaction rate constants at different reaction sites for all the methyl esters studied in this work. The calculated rate constants as a function of temperature at different reaction sites for methyl valerate, methyl-2-pentenoate, methyl-3-pentenoate and methyl-4-pentenoate are shown in figure 6. For methyl valerate, it can be seen that the rate constants at different reaction sites exhibit the following tendency: $\gamma > \alpha > \beta > \delta > \alpha'$, clearly indicating that the rate constant of the primary carbon is less than that of the secondary carbon. For the other three unsaturated linear methyl esters, it is shown that the rate constants at the C=C double bond sites are all lower than that at the other sites. However, it is worth noting that with the presence of the C=C double bond, the reactivity on allylic sites is greatly favored as revealed by the reaction rate constants, which is also revealed by the above potential energy information. The reaction rate constants at the allylic sites for the unsaturated methyl esters are relatively larger than the other reaction sites, especially at low temperatures.

For methyl 2-methylbutanoate and its corresponding three unsaturated methyl esters, namely, methyl tiglate, methyl 2-methylbut-3-enoate, and methyl 2-methylenebutyrate, figure 7 exhibits the rate constants as a function of temperature at different reaction sites. The rate constants at the α site (tertiary carbon) is the largest for methyl 2-methylbutanoate, which is also revealed by the calculated energy barriers. The overall tendency of the rate constants is primary carbon (α', γ and δ sites) < secondary carbon (β site) < tertiary carbon (α site). Further, the rate constants among the three primary carbon sites are close to each other. For methyl tiglate, the rate

constants of the two allylic sites are nearly identical and larger than that of the other sites due to the existence of the C=C donble bond. For methyl 2-methylbut-3-enoate, the rate constants at the α site, also the allylic site of the double bond are the largest. The tendencies of the rate constants at different reaction sites of methyl 2-methylenebutyrate exhibit similar rules: the rate constants at the allylic site (β site) are the largest, the rate constants at the double bond position (δ site) is the lowest, and the rate constants at the other two primary carbon sites (α' and γ sites) are close to each other.

Figure 8 gives the rate constants as a function of temperature for methyl isopentanoate, methyl senecioate and methyl 3-methylbut-3-enoate. The variation tendencies of the rate constants at different sites for methyl isopentanoate are very similar to methyl 2-methylbutanoate, and the rate constants at the β site (tertiary carbon) are the largest as revealed by the calculated energy barriers. The rate constants at the α site (secondary carbon) are larger than that at the tertiary carbon sites. For methyl senecioate and methyl 3-methylbut-3-enoate, with the presence of the C=C double bond, the rate constants of the two allylic sites are larger than that of the other sites. Further, similar to the other unsaturated methyl esters studied in this work, the direct hydrogen abstraction reaction at the C=C donble bond is also difficult compared with the other sites. Tables 4 to 6 list all the fitted reaction rate coefficients in three-parameter Arrhenius expression at different reaction sites for all the methyl esters, which can be used for combustion chemical kinetic modeling studies.

3.3. Branching ratio analysis

The different trends of the rate constants as a function of temperature at different reaction sites for the methyl esters would directly affect the results of combustion chemical kinetic modeling due to the resulting products from the hydrogen abstraction reactions. In order to further understand the chemical kinetics, a branching ratio analysis for all the methyl esters has been carried out in the temperature range 500-2500 K, as shown in figures 9-11. From figure 9, it can be seen that the abstraction reaction at the γ site is dominant at temperature below 1000 K for methyl valerate, and decreases as temperature increases. The abstraction reactions at the α' and δ sites (primary carbon site) increase as temperature rises, but the largest contributions are still within 0.15 even when the temperature increases to 2500 K. The branching ratios of the abstraction reactions at the α and β sites changes gradually over the whole temperature range and the predicted branching ratios are around 0.25 and 0.13, respectively. For the other three unsaturated linear methyl esters, namely, methyl-2-pentenoate, methyl-3-pentenoate and methyl-4-pentenoate, it is obvious that the abstraction reaction at the allylic site completely dominates the branching ratios at low temperature due to the presence of the C=C double bond. The branching ratios at the other sites gradually increase as temperature rises, but the ratios are

almost all less than that at the allylic site.

For methyl 2-methylbutanoate and methyl isopentanoate, the two saturated methyl esters with branched alkyl group, it can be seen that the predicted branching ratio at the tertiary carbon site is dominant and decreases as temperature increases as shown in figures 10 and 11. The branching ratio at the secondary carbon site has little change and the value is a little large than 0.2 over the whole temperature range. Although the branching ratios at the other primary carbon sites increase as temperature rises, the values of the branching ratios are less than that at the secondary and tertiary carbon sites over the whole temperature range. For the other unsaturated methyl esters shown in figures 10 and 11, it can be seen that the variation tendencies of the predicted branching ratios are similar to the three unsaturated linear methyl esters as shown in figure 8. The branching ratio at the allylic site is dominant but decreases as temperature increases. Even though, the branching ratios are still larger than that at the other sites for nearly all the unsaturated methyl esters shown in figures 10 and 11.

4. Conclusions

This work reports a systematic *ab initio* and chemical kinetic study of the rate constants for hydrogen atom abstraction reactions by hydrogen radical on the isomers of unsaturated C6 methyl esters. The high-pressure limit rate constants at every reaction site for all the methyl esters studied in this work are calculated via conventional transition-state theory with the asymmetric Eckart method for quantum tunneling effect by using the accurate potential energy information obtained with the CBS/QB3 method. The low-frequency internal rotations are taken into account as hindered rotor approximations. Further, the thermodynamic properties for all the methyl esters including the enthalpy of formation and entropy at 298 K and the heat capacity at a series of temperatures are also computed, which can be fitted for combustion kinetic modeling studies.

Based on the calculated reaction barrier heights and reaction enthalpies, a linear energy relationship (LER) between the barrier heights and reaction enthalpies at 298 K for the H-abstraction reactions of all the methyl esters with H in this work is found. Through a detailed comparisons of the predicted reaction barrier heights at different reaction sites for saturated methyl esters, it is found that the barrier heights exhibit the following tendency: primary carbon (from 10.1 to 10.4 kcal/mol) > secondary carbon (from 6.8 to 7.6 kcal/mol) > tertiary carbon (from 5.3 to 6.7 kcal/mol). For unsaturated methyl esters, with the presence of the C=C double bond, the hydrogen abstraction reactions on the allylic sites are favored, while the direct hydrogen abstraction reactions at the C=C double bond position is difficult due to the high barrier heights.

When comparing the reaction rate constants at different reaction sites for saturated methyl esters, it is

shown that the hydrogen abstraction reaction at the tertiary carbon is the most active position, and the overall tendency of the rate constants is primary carbon < secondary carbon < tertiary carbon. For unsaturated methyl esters, the rate constants on the allylic sites are the largest among all the reaction sites due to the presence of the C=C double bond. The calculated rate constants at every reaction site for all the methyl esters studied in the present work have been fitted into the modified three parameters Arrhenius expression, which is compatible with the Chemkin software and can be directly used in combustion chemical kinetic modeling.

Electronic supplementary information (ESI) available: Optimized geometries and vibrational frequenices at the B3LYP/6-311G(2d,d,p) level for all the stationary points on the potential energy surfaces.

Acknowledgments

This work is supported by the Fundamental Research Funds for the Central Universities of China (Nos. 2013QNA08 and 2014ZDPY20) and the National Natural Science Foundation of China (No. 21403296). We also thank National Supercomputing Center in Shenzhen for providing the computational resources and Gaussian 09 suite of programs (Revision D.01).

References

1. K. Kohse-Höinghaus, P. Oßwald, T. A. Cool, T. Kasper, N. Hansen, F. Qi, C. K. Westbrook and P. R. Westmoreland, *Angew. Chem. Int. Ed.,* 2010, 49, 3572-3597.
2. M. M. Rashed, M. A. Kalam, H. H. Masjuki, H. K. Rashedul, A. M. Ashraful, I. Shancita and A. M. Ruhul, *RSC Adv.,* 2015, 5, 36240-36261.
3. L. Coniglio, H. Bennadji, P. A. Glaude, O. Herbinet and F. Billaud, *Prog. Energy Combust. Sci.,* 2013, 39, 340-382.
4. J. Y. W. Lai, K. C. Lin and A. Violi, *Prog. Energy Combust. Sci.,* 2011, 37, 1-14.
5. Q. Feng, A. Jalali, A. M. Fincham, Y. L. Wang, T. T. Tsotsis and F. N. Egolfopoulos, *Combust. Flame,* 2012, 159, 1876-1893.
6. S. Sarathy, S. Gaïl, S. Syed, M. Thomson and P. Dagaut, *Proc. Combust. Inst.,* 2007, 31, 1015-1022.
7. S. Gaïl, S. Sarathy, M. Thomson, P. Diévart and P. Dagaut, *Combust. Flame,* 2008, 155, 635-650.
8. B. Yang, C. K. Westbrook, T. A. Cool, N. Hansen and K. Kohse-Höinghaus, *Proc. Combust. Inst.,* 2013, 34, 443-451.
9. K. Zhang, C. Togbé, G. Dayma and P. Dagaut, *Combust. Flame,* 2014, 161, 818-825.
10. D. D. Das, C. S. McEnally and L. D. Pfefferle, *Combust. Flame,* 2015, 162, 1489-1497.
11. O. Herbinet, W. J. Pitz and C. K. Westbrook, *Combust. Flame,* 2010, 157, 893-908.
12. C. K. Westbrook, C. V. Naik, O. Herbinet, W. J. Pitz, M. Mehl, S. M. Sarathy and H. J. Curran, *Combust. Flame,* 2011, 158, 742-755.

13. C. V. Naik, C. K. Westbrook, O. Herbinet, W. J. Pitz and M. Mehl, *Proc. Combust. Inst.,* 2011, 33, 383-389.
14. C. K. Westbrook, W. J. Pitz, S. M. Sarathy and M. Mehl, *Proc. Combust. Inst.,* 2013, 34, 3049-3056.
15. A. Fridlyand, S. S. Goldsborough and K. Brezinsky, *J. Phys. Chem. A,* 2015, 119, 7559-7577.
16. Q.-D. Wang, *RSC Adv.,* 2014, 4, 4564-4585.
17. J. Zádor, C. A. Taatjes and R. X. Fernandes, *Prog. Energy Combust. Sci.,* 2011, 37, 371-421.
18. Q.-D. Wang, X.-J. Wang and G.-J. Kang, *Comput. Theor. Chem.,* 2014, 1027, 103-111.
19. Q.-D. Wang, X.-J. Wang, Z.-W. Liu, G.-J. Kang, *Chem. Phys. Lett.,* 2014, 616-617, 109-114.
20. J. Mendes, C.-W. Zhou and H. J. Curran, *J. Phys. Chem. A* 2013, 117, 14006-14018.
21. L. Zhang, Q. Chen and P. Zhang, *Proc. Combust. Inst.,* 2015, 35, 481-489.
22. J. Mendes, C.-W. Zhou and H. J. Curran, *J. Phys. Chem. A* 2014, 118, 4889-4899.
23. X. T. Le, T. V. T. Mai, A. Ratkiewicz and L. K. Huynh, *J. Phys. Chem. A* 2015, 119, 3689-3703.
24. M. A. Ali and A. Violi, *J. Org. Chem.,* 2013, 78, 5898-5908.
25. M. J. Frisch, G. W. Trucks, H. B. Schlegel, G. E. Scuseria, M. A. Robb, J. R. Cheeseman, J. A. Montgomery, T. Vreven, K. N. Kudin, J. C. Burant, J. M. Millam, S. S. Iyengar, J. Tomasi, V. Barone, B. Mennucci, M. Cossi, G. Scalmani, N. Rega, G. A. Petersson, H. Nakatsuji, M. Hada, M. Ehara, K. Toyota, R. Fukuda, J. Hasegawa, M. Ishida, T. Nakajima, Y. Honda, O. Kitao, H. Nakai, M. Klene, X. Li, J. E. Knox, H. P. Hratchian, J. B. Cross, V. Bakken, C. Adamo, J. Jaramillo, R. Gomperts, R. E. Stratmann, O. Yazyev, A. J. Austin, R. Cammi, C. Pomelli, J. W. Ochterski, P. Y. Ayala, K. Morokuma, G. A. Voth, P. Salvador, J. J. Dannenberg, V. G. Zakrzewski, S. Dapprich, A. D. Daniels, M. C. Strain, O. Farkas, D. K. Malick, A. D. Rabuck, K. Raghavachari, J. B. Foresman, J. V. Ortiz, Q. Cui, A. G. Baboul, S. Clifford, J. Cioslowski, B. B. Stefanov, G. Liu, A. Liashenko, P. Piskorz, I. Komaromi, R. L. Martin, D. J. Fox, T. Keith, A. Laham, C. Y. Peng, A. Nanayakkara, M. Challacombe, P. M. W. Gill, B. Johnson, W. Chen, M. W. Wong, C. Gonzalez and J. A. Pople, Gaussian 09, Revision D.01., Gaussian, Inc., Wallingford CT, 2013.
26. J. A. Montgomery, M. J. Frisch, J. W. Ochterski and G. A. Petersson, *J. Chem. Phys.,* 1999, 110, 2822-2827.
27. C. Gonzalez and H. B. Schlegel, *J. Phys. Chem.,* 1990, 94, 5523-5527.
28. K. S. Pitzer, *J. Chem. Phys.,* 1946, 14, 239-243.
29. A. L. L. East and L. Radom, *J. Chem. Phys.,* 1997, 106, 6655-6674.
30. R. B. McClurg, R. C. Flagan and W. A. Goddard III., *J. Chem. Phys.,* 1997, 106, 6675-6680.
31. S. Sharma, M. R. Harper, W. H. Green, CANTHERM, http://sourceforge.net/projects/cantherm, 2010.
32. S. Glasstone, K. J. Laidler and H. Eyring, The theory of rate processes, McGraw-Hill: New York, 1941.
33. S. Canneaux, F. Bohr and E. Henon, *J. Comput. Chem.,* 2014, 35, 82-93.

34. L. A. Curtiss, K. Raghavachari, P. C. Redfern and J. A. Pople, *J. Chem. Phys.,* 1997, 106, 1063-1079.

35. E. Papajak and D. G. Truhlar, *J. Chem. Phys.,* 2012, 137, 064110.

36. C. F. Goldsmith, G. R. Magoon and W. H. Green, *J. Phys. Chem. A,* 2012, 116, 9033-9057.

37. L. Zhang, P. Zhang, *Phys. Chem. Chem. Phys.,* 2015,17, 200-208.

38. A. Fernández-Ramos, J. A. Miller, S. J. Klippenstein and D. G. Truhlar, *Chem. Rev.,* 2006, 106, 4518-4584.

39. C. Eckart, *Phys. Rev.,* 1930, 35, 1303-1909.

40. H. S. Johnston and J. Heicklen, *J. Phys. Chem.,* 1962, 66, 532-533.

41. B. Sirjean, E. Dames, H. Wang and W. Tsang, *J. Phys. Chem. A,* 2012, 116, 319-332.

42. T. Tan, X. Yang, C. M. Krauter, Y Ju and E. A. Carter, *J. Phys. Chem. A,* 2015, 119, 6377-6390.

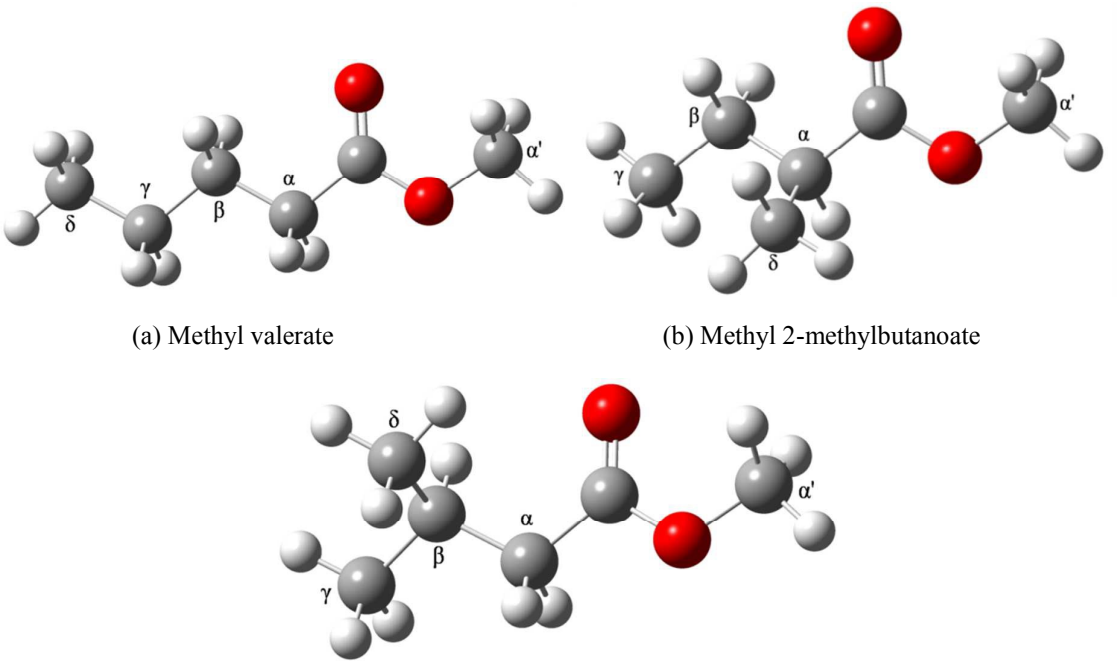

(a) Methyl valerate (b) Methyl 2-methylbutanoate

(c) Methyl isopentanoate

Fig. 1 Labels used in this work.

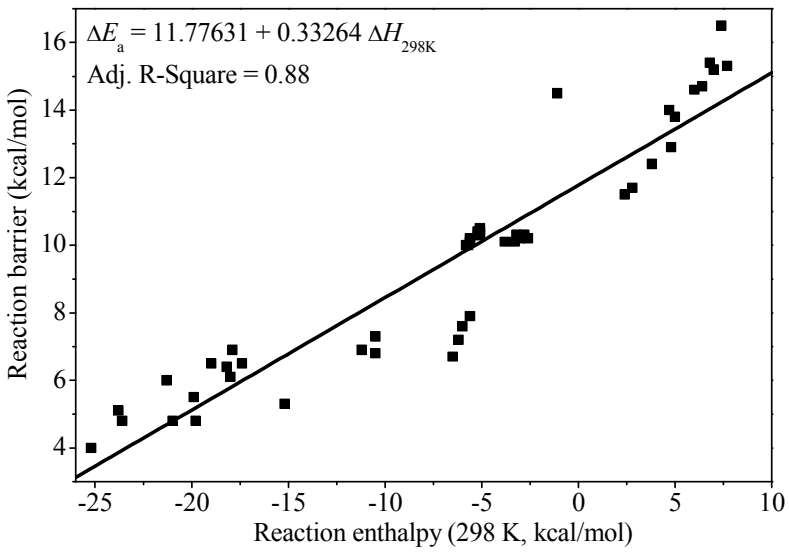

Fig. 2 Linear energy relationship plot of the energy barriers versus the reaction enthalpy.

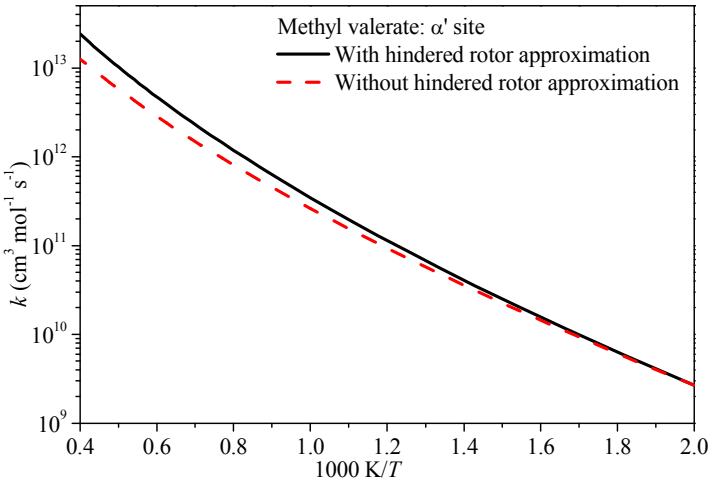

Fig. 3 The effect of the low frequency internal rotations on the calculated rate constants.

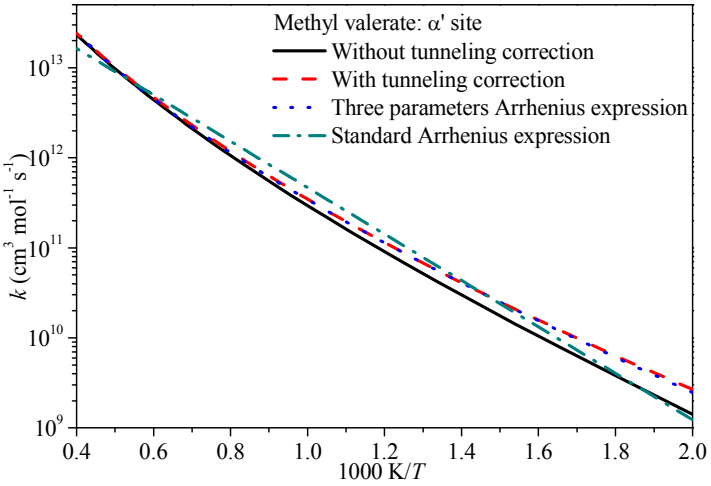

Fig. 4 The effect of the tunneling effect on the calculated rate constants.

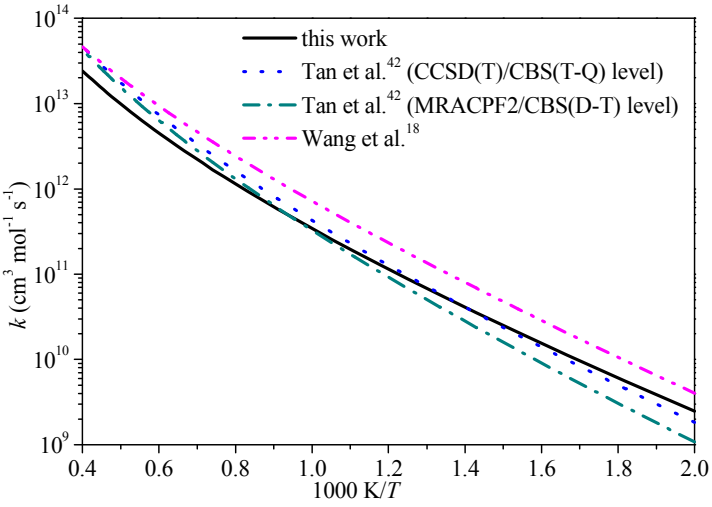

Fig. 5 Comparisons of predicted rate constants (this work) with available results from the literature.

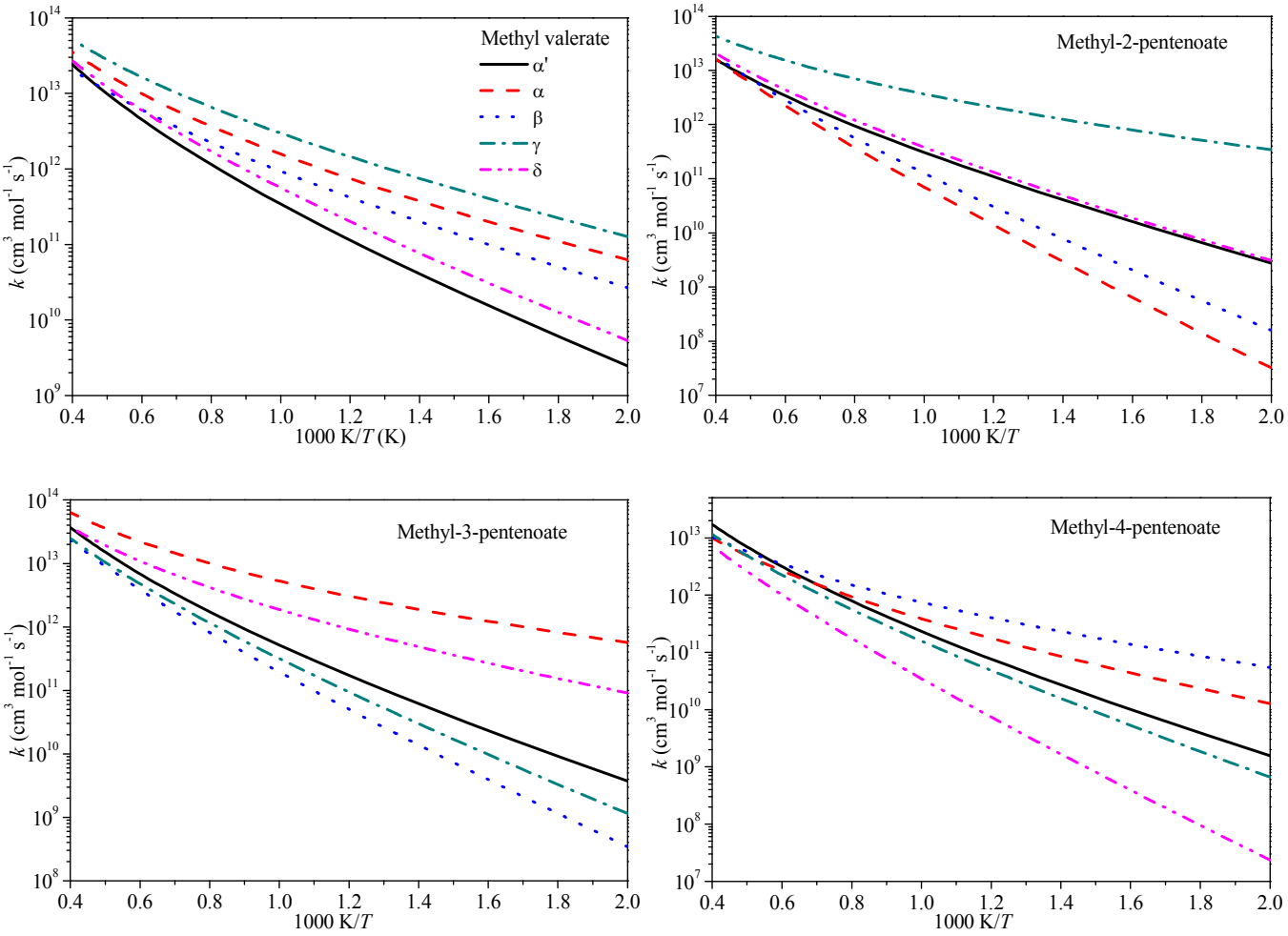

Fig. 6 Rate constants as a function of temperature at different reaction sites for methyl valerate, methyl-2-pentenoate, methyl-3-pentenoate and methyl-4-pentenoate.

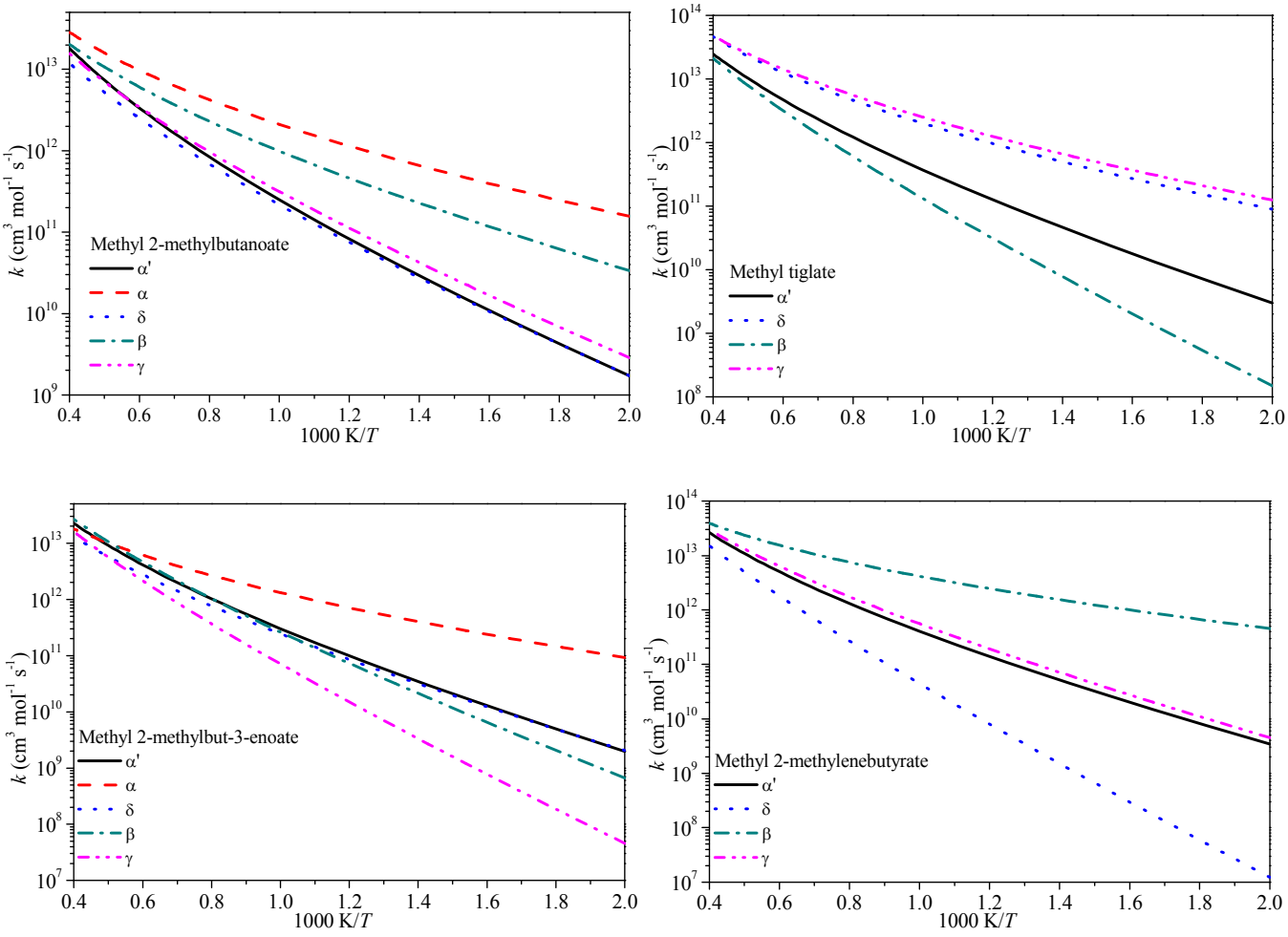

Fig. 7 Rate constants as a function of temperature at different reaction sites for methyl 2-methylbutanoate, methyl tiglate, methyl 2-methylbut-3-enoate, and methyl 2-methylenebutyrate.

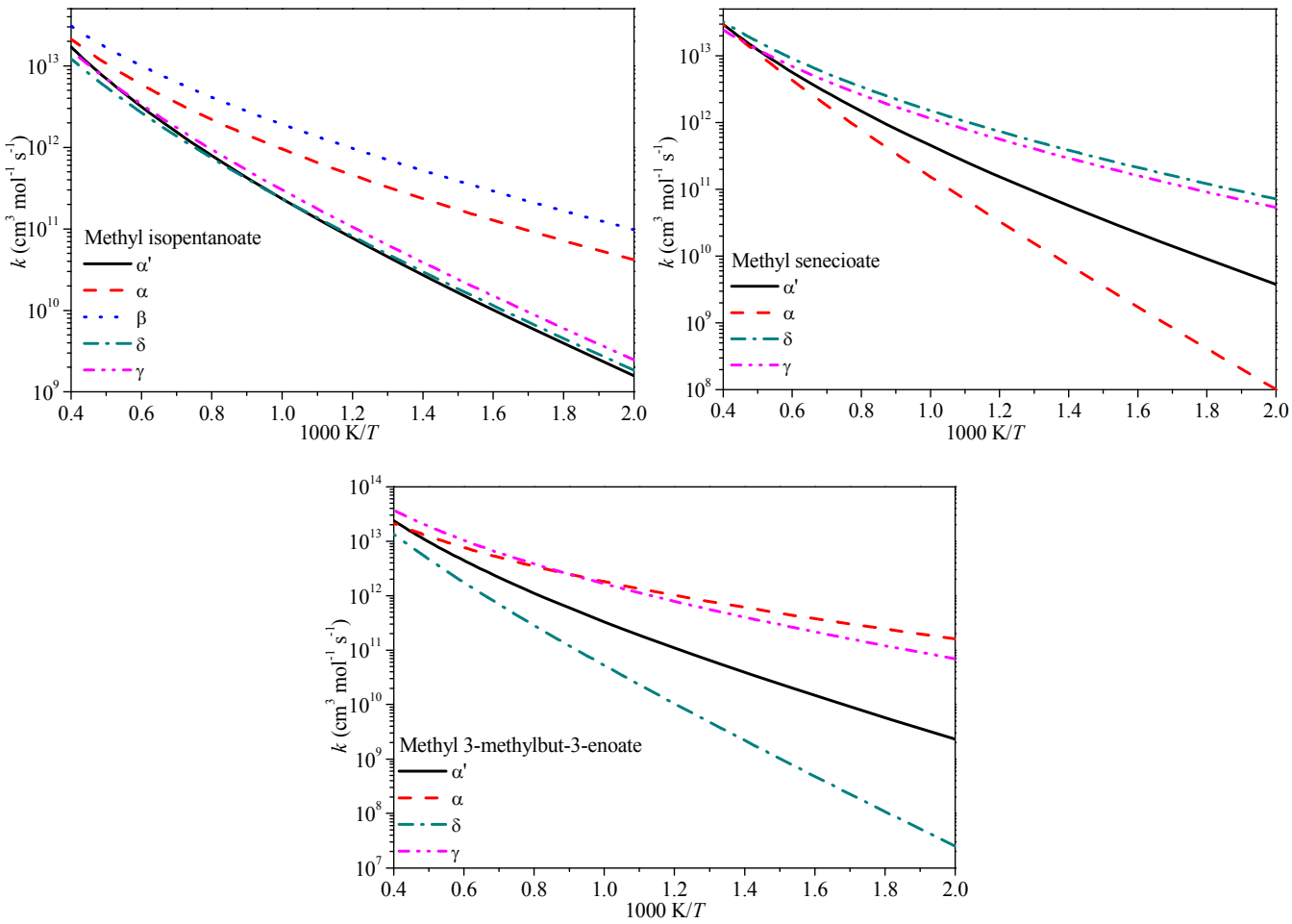

Fig. 8 Rate constants as a function of temperature at different reaction sites for methyl isopentanoate, methyl senecioate and methyl 3-methylbut-3-enoate.

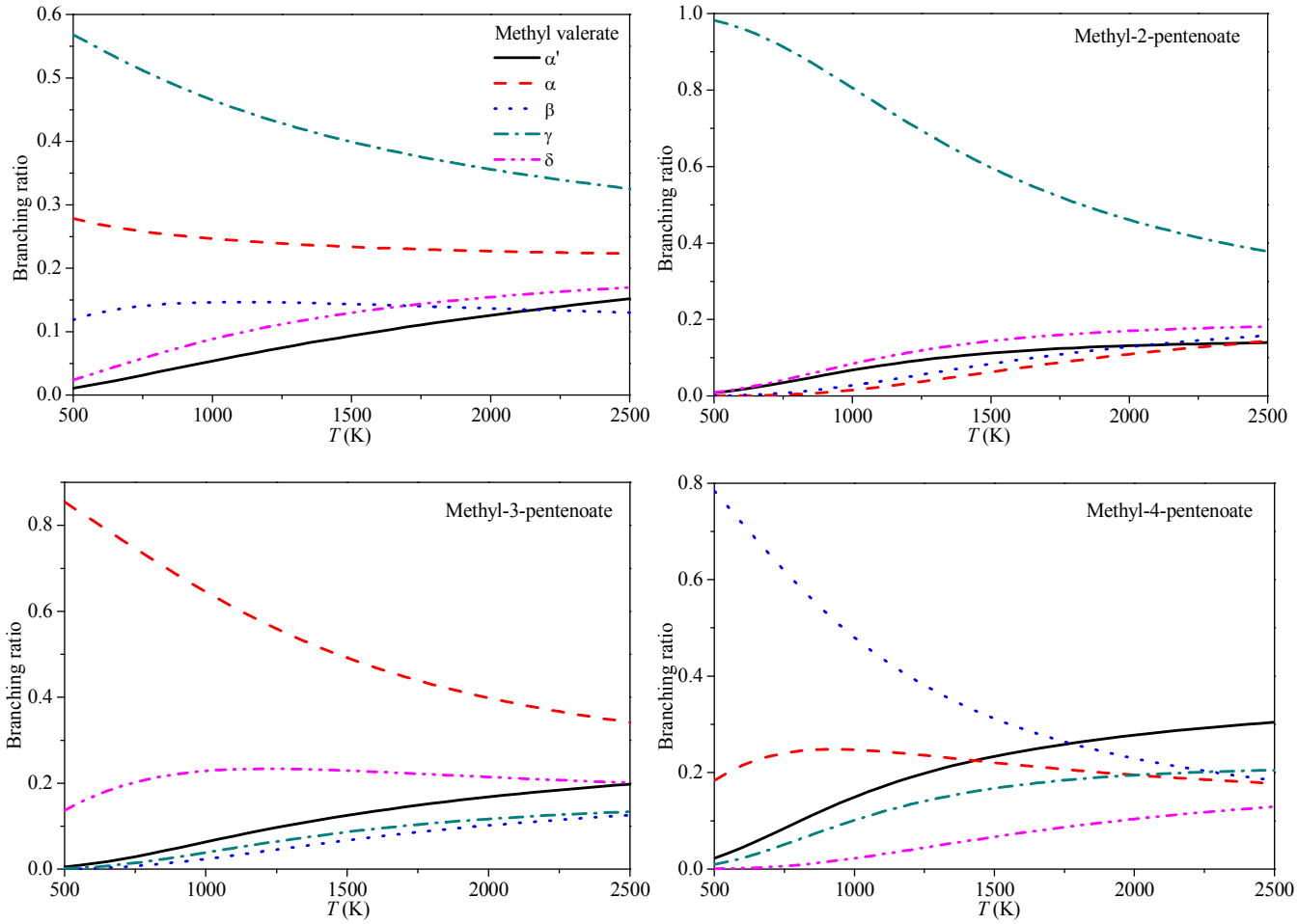

Fig. 9 Predicted branching ratios for the different sites of methyl valerate, methyl-2-pentenoate, methyl-3-pentenoate and methyl-4-pentenoate, between 500 and 2500 K.

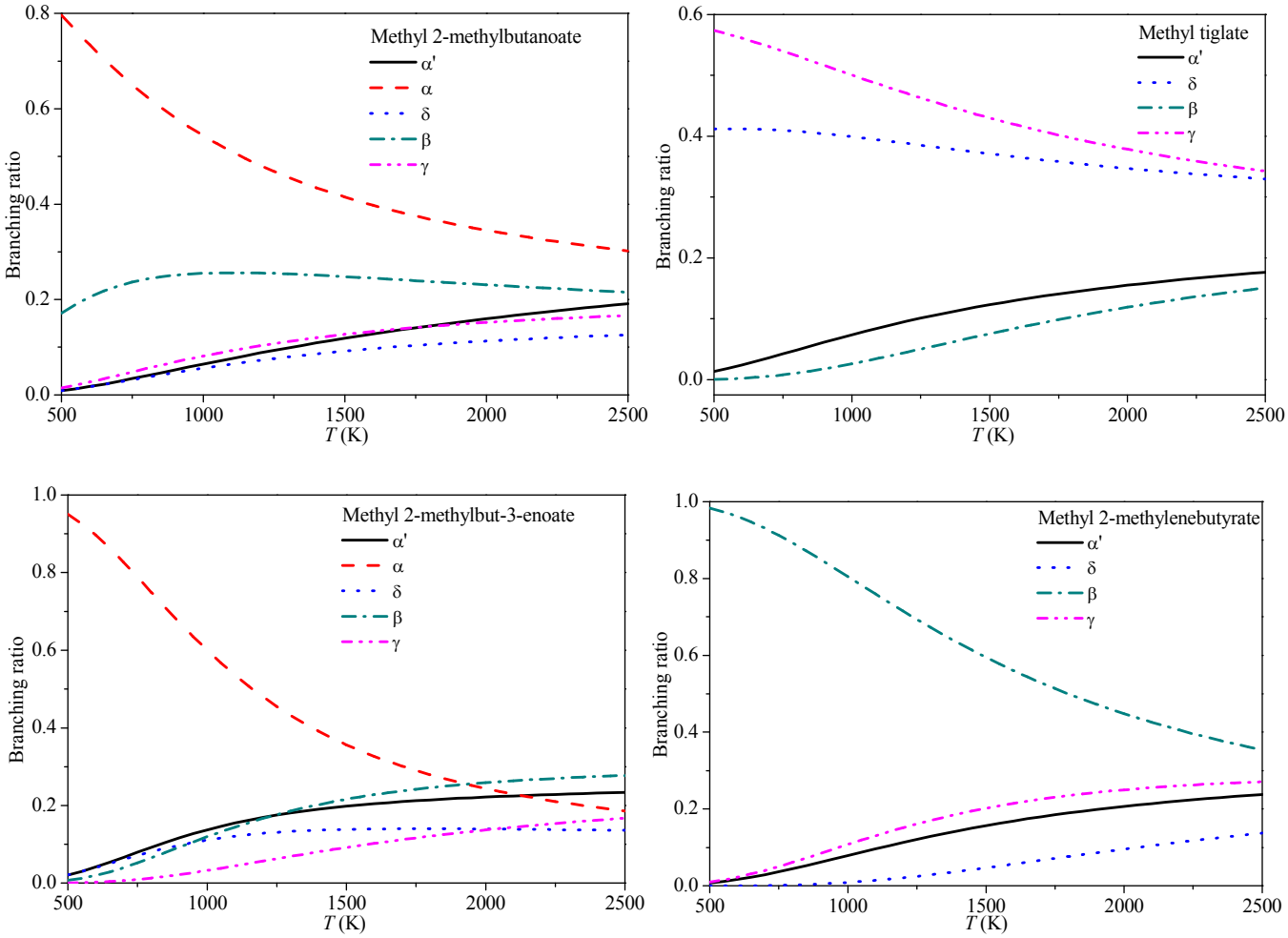

Fig. 10 Predicted branching ratios for the different sites of methyl 2-methylbutanoate, methyl tiglate, methyl 2-methylbut-3-enoate, and methyl 2-methylenebutyrate, between 500 and 2500 K.

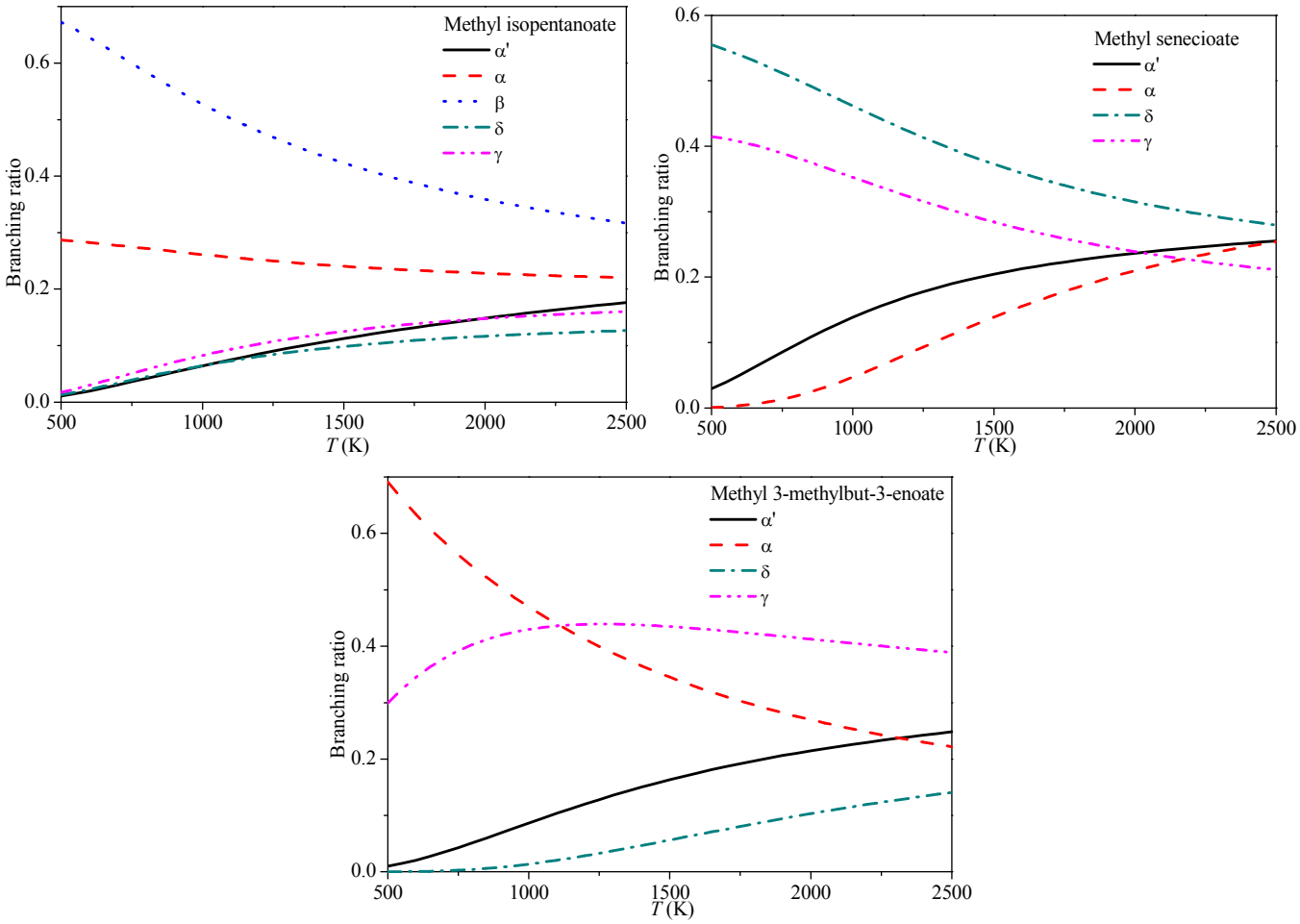

Fig. 11 Predicted branching ratios for the different sites of methyl isopentanoate, methyl senecioate and methyl 3-methylbut-3-enoate, between 500 and 2500 K.

Table 1 Species thermochemistry properties, calculated using CBS-QB3 with 1-D hindered rotor corrections.[a]

Species	$\Delta_f H^o_{298K}$	S^o_{298K}	$C_p^o(T)$						
			300 K	400 K	500 K	600 K	800 K	1000 K	1500 K
Methyl valerate	-113.4 (-112.8)[b]	100.88	37.60	46.07	54.12	61.20	72.63	81.22	94.13
Methyl-2-pentenoate	-86.1	101.42	39.78	47.21	54.07	60.11	69.94	77.26	87.79
Methyl-3-pentenoate	-84.6	104.51	38.61	45.79	52.54	58.58	68.48	75.90	86.78
Methyl-4-pentenoate	-82.9	109.25	40.56	47.32	53.71	59.39	68.75	75.88	86.51
Methyl 2-methylbutanoate	-114.2 (-117.7±1.8)[b]	112.33	42.65	50.76	58.14	64.56	75.01	83.02	95.26
Methyl tiglate	-88.3	111.81	39.56	46.56	53.23	59.13	68.72	75.94	86.89
Methyl 2-methylbut-3-enoate	-83.6	106.55	40.27	47.00	53.39	59.11	68.59	75.84	86.68
Methyl 2-methylenebutyrate	-85.9	108.79	40.66	48.15	54.98	60.88	70.26	77.22	87.66
Methyl isopentanoate	-115.5 (-119.0±1.8)[b]	109.23	44.22	52.39	59.80	66.26	76.73	84.60	96.27
Methyl senecioate	-89.2	106.85	40.89	48.21	54.87	60.73	70.25	77.37	87.69
Methyl 3-methylbut-3-enoate	-84.6	108.45	40.51	47.10	53.40	59.07	68.50	75.67	86.29

[a]Enthalpy has units of kcal mol^{-1}; entropy and heat capacity have units of cal mol^{-1} K^{-1}.

[b]Experimantal results from NIST Chemistry WebBook.

Table 2 Calculated energy barriers and reaction enthalpies for methyl valerate (Units: kcal/mol).

Methyl valerate	Energy barrier		Reaction enthalpy (298 K)	
	Present work	Ref. 37	Present work	Ref. 37
α'	10.3	10.35	-5.2	-5.52
α	6.9	7.05	-11.2	-10.39
β	7.9	8.20	-5.6	-5.66
γ	7.2	7.54	-6.2	-6.34
δ	10.1	10.26	-3.3	-3.51

Table 3 Theoretical predicted energy barriers and reaction enthalpies for all the reactions (Units: kcal/mol).

Methyl esters	Structure	Energy barrier				Reaction enthalpy (298 K)					
		α'	α	β	γ	δ	α'	α	β	γ	δ
Methyl valerate	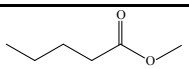	10.3	6.9	7.9	7.2	10.1	-5.2	-11.2	-5.6	-6.2	-3.3
Methyl-2-pentenoate	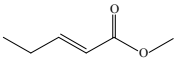	10.2	15.3	13.8	4.8	10.3	-5.6	7.7	5.0	-23.6	-2.8
Methyl-3-pentenoate	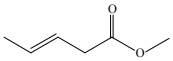	10.3	4.0	12.9	11.7	6.4	-5.1	-25.2	4.8	2.8	-18.2
Methyl-4-pentenoate	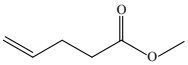	10.4	7.3	5.5	11.5	14.6	-5.1	-10.5	-19.9	2.4	6.0
Methyl 2-methylbutanoate	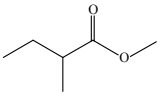	10.4	5.3	7.6	10.1	10.3	-5.2	-15.2	-6.0	-3.8	-3.2
Methyl tiglate	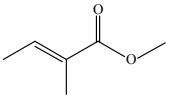	10.1	—	14.0	6.0	6.5	-5.6	—	4.7	-21.3	-17.4
Methyl 2-methylbut-3-enoate	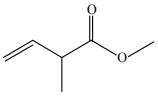	10.5	5.1	12.4	14.7	10.2	-5.1	-23.8	3.8	6.4	-2.6
Methyl 2-methylenebutyrate	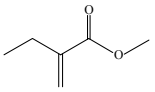	10.0	—	4.8	10.3	16.5	-5.7	—	-19.8	-3.2	7.4
Methyl isopentanoate	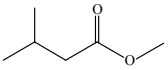	10.4	6.8	6.7	10.2	10.3	-5.2	-10.5	-6.5	-3.0	-2.8
Methyl senecioate	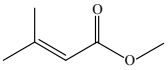	10.0	14.5	—	6.5	6.1	-5.8	-1.1	—	-19.0	-18.0
Methyl 3-methylbut-3-enoate	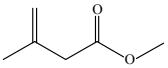	10.4	4.8	—	6.9	15.2	-5.2	-21.0	—	-17.9	7.0

Table 4 Fitted rate coefficients for the different abstraction positions of the esters. (A: cm^3 mol^{-1} s^{-1}, E_a: kcal mol^{-1})

Site	Methyl valerate			Methyl-2-pentenoate			Methyl-3-pentenoate			Methyl-4-pentenoate		
	A	n	E_a	A	n	E_a	A	n	E_a	A	n	E_a
α'	1.34×10^{5}	2.59	6.23	1.37×10^{6}	2.24	6.26	1.89×10^{5}	2.60	6.23	9.78×10^{4}	2.59	6.38
α	6.41×10^{5}	2.36	3.16	5.08×10^{8}	1.66	12.99	1.26×10^{6}	2.30	1.26	1.29×10^{5}	2.41	3.46
β	1.39×10^{7}	1.93	4.41	5.84×10^{7}	1.89	10.68	3.17×10^{7}	1.98	9.85	1.21×10^{6}	2.10	2.32
γ	2.72×10^{7}	1.94	3.58	5.32×10^{6}	2.08	1.84	2.55×10^{7}	1.98	8.44	8.03×10^{6}	2.02	8.09
δ	4.37×10^{6}	2.16	6.27	2.58×10^{6}	2.20	6.54	6.23×10^{5}	2.36	2.76	2.18×10^{7}	1.93	11.84

Table 5 Fitted rate coefficients for the different abstraction positions of the esters. (A: cm^3 mol^{-1} s^{-1}, E_a: kcal mol^{-1})

Site	Methyl 2-methylbutanoate			Methyl tiglate			Methyl 2-methylbut-3-enoate			Methyl 2-methylenebutyrate		
	A	n	E_a	A	n	E_a	A	N	E_a	A	n	E_a
α'	1.02×10^5	2.59	6.33	1.22×10^5	2.60	6.02	1.29×10^5	2.59	6.41	1.17×10^5	2.61	5.89
α	3.31×10^6	2.10	2.27	—	—	—	4.39×10^6	2.01	2.53	—	—	—
β	7.23×10^6	2.00	3.96	2.72×10^7	2.01	10.72	1.51×10^7	2.07	9.02	3.19×10^7	1.84	1.85
γ	2.20×10^6	2.18	6.34	1.40×10^6	2.29	2.82	2.37×10^7	2.02	11.82	3.75×10^6	2.20	6.53
δ	1.38×10^6	2.21	6.56	1.86×10^5	2.54	2.68	1.36×10^6	2.22	6.44	1.74×10^8	1.81	13.82

Table 6 Fitted rate coefficients for the different abstraction positions of the esters. (A: cm^3 mol^{-1} s^{-1}, E_a: kcal mol^{-1})

Site	Methyl isopentanoate			Methyl senecioate			Methyl 3-methylbut-3-enoate		
	A	n	E_a	A	n	E_a	A	n	E_a
α'	1.06×10^5	2.58	6.38	1.32×10^5	2.61	5.92	1.34×10^5	2.59	6.30
α	1.52×10^5	2.47	2.81	5.32×10^8	1.71	12.21	3.73×10^6	2.04	1.99
β	1.18×10^7	1.97	3.21	—	—	—	—	—	—
γ	3.40×10^6	2.13	6.60	2.56×10^5	2.42	2.77	3.45×10^5	2.44	2.93
δ	3.48×10^6	2.10	6.73	2.24×10^5	2.47	2.66	4.67×10^7	1.93	12.53

This work reports a systematic *ab initio* and chemical kinetic study of the rate constants for hydrogen atom abstraction reactions by hydrogen radical on the isomers of unsaturated C6 methyl esters.